Spin dynamics in doped triangular antiferromagnets

Pengpeng Zhang and Shiping Feng
Department of Physics, Beijing Normal University, Beijing 100875, China

Wei Yeu Chen
Department of Physics, Tamkang University, Tamsui 25137, Taiwan
(Received 20 June 2000)

Within the t–J model, the spin response of the doped triangular antiferromagnet in the underdoped and optimally doped regimes is studied based on the fermion-spin theory. The spinon part is treated by using the loop expansion to the second order. It is shown that although the dynamical spin structure factor and susceptibility exhibit the anomalous behaviors at the antiferromagnetic zone center, the particularly universal behaviors of the integrated dynamical spin structure factor and susceptibility present in the doped square antiferromagnet, are absent in the doped triangular antiferromagnet.

In the last decade, much interest has focused on the magnetic properties of the two-dimensional (2D) doped antiferromagnets.[1] This is followed from the argument that the essential physics of copper oxide materials is contained in the 2D doped Mott insulators,[2] since all of copper oxide materials have these properties in common: their perovskite parent compound is insulating with the antiferromagnetic (AF) long-range order (AFLRO); changing the carrier concentration by ionic substitution or increasing the oxygen content turns these compounds into correlated metals leaving the short-range AF correlation still intact.[1,3] In the underdoped and optimally doped regimes, the short-range correlation is responsible for the nuclear magnetic resonance (NMR) and nuclear quadrupole resonance (NQR).[1,3] In particular, a series of the neutron-scattering measurements[4–7] on copper oxide materials show that there is an anomalous temperature T dependence of the spin fluctuation near the AF zone center in the underdoped and optimally doped regimes, and the low-frequency integrated dynamical spin susceptibility follows a surprisingly simple scaling function as $\chi''(\omega)\propto\arctan(\omega/T)$. These unusual magnetic properties of copper oxide materials result from special microscopic conditions:[1,3] (1) Cu ions situated in a square-planar arrangement and bridged by oxygen ions, (2) weak coupling between neighboring layers, and (3) doping in such a way that the Fermi level lies near the middle of the Cu–O σ^* bond. One common feature of these compounds is the *square-planar* Cu arrangement. However, it has been reported[8] that there is a class of the delafossite copper oxide materials, $R\mathrm{CuO}_{2+\delta}$ with R as rare-earth element, where the Cu ions sit not on a square-planar, but on a *triangular-planar lattice*, therefore allowing a test of the geometry effect on the physical properties, while retaining some other unique microscopic features of the Cu–O bond. In other words, whether the particularly anomalous magnetic behaviors observed on the doped square antiferromagnet are also true in the doped triangular antiferromagnet. On the other hand, the magnetic properties of the undoped triangular antiferromagnet have been extensively studied,[9] and the results show that the deviation of the spin susceptibility from the Curie law occurs at a much lower temperature than for the nonfrustrated square antiferromagnet, and is often accompanied by very peculiar low-temperature properties. Recognizing these anomalous magnetic properties shown by the undoped triangular antiferromagnet, a natural question is what is the magnetic property with doping on this system?

The situation for the doped square antiferromagnet is a bit more advanced. The spin dynamics of the doped square antiferromagnet in the underdoped and optimally doped regimes has been extensively studied experimentally[4–7] as well as theoretically within the same strongly correlated electron models,[10–12] and the results show that the unusual spin dynamics in the doped square antiferromagnet is caused by the strong electron correlation. Among the microscopic models the most helpful for the discussion of the physical properties of the doped antiferromagnet is the t–J model,[2] which is characterized by a competition between the kinetic energy (t) and magnetic energy (J). The t–J model was originally introduced as an effective Hamiltonian of the Hubbard model in the strong coupling regime,[2] where the on-site Coulomb repulsion U is very large as compared with the electron kinetic energy t, and in this case the electrons become strongly correlated to avoid the double occupancy, i.e., $\Sigma_\sigma C^+_{i\sigma}C^-_{i\sigma}\leqslant 1$. Since the strong electron correlations are common for both doped square and triangular antiferromagnets, it is expected that the unconventional spin dynamics observed on the doped square antiferromagnet may also be seen in the doped triangular antiferromagnet. Following the common practice, the regimes in the doped triangular antiferromagnet can be classified into the underdoped, optimally doped, and overdoped, respectively, as in the case of the doped square antiferromagnet, although the boundary of these regimes in the doped triangular antiferromagnet may be different from the doped square antiferromagnet. In this paper, we study the spin dynamics of the doped triangular antiferromagnet in the underdoped and optimally doped regimes within the t–J model.

In the t–J model, the strong electron correlation manifests itself by the electron single occupancy on-site local constraint, which can be treated exactly in analytical calculations within the fermion-spin theory based on the charge-spin separation.[13,14] Therefore we follow the fermion-spin formalism and decompose the constrained electron operators in the doped antiferromagnet as[13] $C_{i\uparrow}=h^\dagger_i S^-_i$ and $C_{i\downarrow}=h^\dagger_i S^+_i$, where the spinless fermion operator h_i describes the charge (holon) degrees of freedom, while the pseudospin operator S_i describes the spin (spinon) degrees of freedom.

In this case, the low energy behavior of the t–J model on the triangular lattice in the fermion-spin representation can be written as[12,13]

$$H=-t\sum_{i\hat{\eta}} h_i h^\dagger_{i+\hat{\eta}}(S^+_i S^-_{i+\hat{\eta}}+S^-_i S^+_{i+\hat{\eta}}) +\mu\sum_i h^\dagger_i h_i + J_{\rm eff}\sum_{i\hat{\eta}} S_i\cdot S_{i+\hat{\eta}}, \quad (1)$$

where the summation is over all sites i, and for each i, over its nearest-neighbor $\hat{\eta}$, $J_{\rm eff}=[(1-\delta)^2-\phi^2]$, δ is the hole doping concentration, $\phi=\langle h^\dagger_i h_{i+\hat{\eta}}\rangle$ is the holon particle-hole order parameter, and μ is the chemical potential. The Hamiltonian (1) contains the holon–spinon interaction, and therefore the spinon and holon are strongly coupled. At the half-filling, the t–J model (1) is reduced as the Heisenberg model. Although it has been shown[15] unambiguously that as in the square lattice, there is indeed AFLRO in the ground state of the AF Heisenberg model on the triangular lattice, this AFLRO should be decreased rapidly with increasing dopings than that on the square lattice due to the geometric frustration, so in both the underdoped and optimally doped regimes, there is no AFLRO for the doped triangular antiferromagnet, i.e., $\langle S^z_i\rangle=0$. Then in the following discussions, we will study the frustrated spinon moves in the background of holons.

Since the basic low-energy excitations are holons and spinons in the framework of the charge-spin separation, it has been shown that the scattering of holons dominates the charge dynamics of the doped antiferromagnet.[16] However, it has also been shown[12] that the spin fluctuations couple only to spinons and therefore no composition law is required in discussing the spin dynamics, but the effect of holons still is considered through the holon's order parameter ϕ entering in the spinon propagator. In this case, the spin dynamics of the doped square antiferromagnet in the underdoped and optimally doped regimes has been discussed[12] within the fermion-spin theory[13,14] by considering the spin fluctuation around the mean-field solution, where the spinon part is treated by the loop expansion to the second order. The results show that the dynamical spin structure factor spectrum of the doped square antiferromagnet at the AF wave vector is separated as low- and high-frequency parts, respectively, but the high-frequency part is suppressed in the dynamical spin susceptibility spectrum $\chi''(Q,\omega)$, while the low-frequency part is the temperature dependent. Moreover, the integrated dynamical spin structure factor is almost temperature independent, the integrated susceptibility shows the particularly universal behavior as $(1/N)\sum_k\chi''(k,\omega)\propto\arctan[a_1\omega/T+a_3(\omega/T)^3]$. These results are consistent with experiments[4–7] from copper oxide materials and numerical simulations.[10] Following their discussions,[12] we can obtain the dynamical spin structure factor and susceptibility for the doped triangular antiferromagnet as

$$S(k,\omega)={\rm Re}\int_0^\infty dt\, e^{i\omega(t-t')}D(k,t-t') =2[1+n_B(\omega)]{\rm Im}\,D(k,\omega), \quad (2a)$$

$$\chi''(k,\omega)=(1-e^{-\beta\omega})S(k,\omega)=2\,{\rm Im}\,D(k,\omega), \quad (2b)$$

respectively, where the full spinon Green's function, $D^{-1}(k,\omega)=D^{(0)-1}(k,\omega)-\Sigma^{(2)}_s(k,\omega)$, with the mean-field spinon Green's function $D^{(0)-1}(k,\omega)=(\omega^2-\omega^2_k)/B_k$, and the second-order spinon self-energy from the holon pair bubble,

$$\Sigma^{(2)}_s(k,\omega)=-\left(\frac{Zt}{N}\right)^2\sum_{pp'}(\gamma_{k-p}+\gamma_{p'+p+k})^2\frac{B_{k+p'}}{\omega_{k+p'}} \times\left(\frac{F_1(k,p,p')}{\omega+\xi_{p+p'}-\xi_p+\omega_{k+p'}+i0^+} -\frac{F_2(k,p,p')}{\omega+\xi_{p+p'}-\xi_p-\omega_{k+p'}+i0^+}\right), \quad (3)$$

where $B_k=\Delta[(2\epsilon\chi_z+\chi)\gamma_k-(\epsilon\chi+2\chi_z)]$, $\Delta=2ZJ_{\rm eff}$, $\epsilon=1+2t\phi/J_{\rm eff}$, $\gamma_k=[\cos k_x+2\cos(k_x/2)\cos(\sqrt{3}k_y/2)]/3$, Z is the number of the nearest-neighbor sites, $F_1(k,p,p')=n_F(\xi_{p+p'})[1-n_F(\xi_p)]+[1+n_B(\omega_{k+p'})][n_F(\xi_p)-n_F(\xi_{p+p'})]$, $F_2(k,p,p')=n_F(\xi_{p+p'})[1-n_F(\xi_p)]-n_B(\omega_{k+p'})[n_F(\xi_p)-n_F(\xi_{p+p'})]$, $n_F(\xi_k)$ and $n_B(\omega_k)$ are the Fermi and Bose distribution functions, respectively, the mean-field holon excitation spectrum $\xi_k=2\chi tZ\gamma_k-\mu$, and mean-field spinon excitation spectrum,

$$\omega^2(k)=\Delta^2[\alpha(C_z-\epsilon\chi_z\gamma_k)-\alpha\epsilon\chi/(2Z)+(1-\alpha)/(4Z)](1-\epsilon\gamma_k) +\Delta^2[\alpha\epsilon(C-\chi\gamma_k-2\chi_z/Z)/2+\epsilon(1-\alpha)/(4Z)]\times(\epsilon-\gamma_k), \quad (4)$$

where the spinon correlation functions $\chi=\langle S^+_i S^-_{i+\hat{\eta}}\rangle$, $C=(1/Z^2)\sum_{\hat{\eta}\hat{\eta}'}\langle S^+_{i+\hat{\eta}}S^-_{i+\hat{\eta}'}\rangle$, $\chi_z=\langle S^z_i S^z_{i+\hat{\eta}}\rangle$, $C_z=(1/Z^2)\sum_{\hat{\eta}\hat{\eta}'}\langle S^z_{i+\hat{\eta}}S^z_{i+\hat{\eta}'}\rangle$. In order not to violate the sum rule $\langle S^+_i S^-_i\rangle=1/2$ for the case $\langle S^z_i\rangle=0$, an important decoupling parameter α has been introduced, which is regarded as the vertex correction.[14,12] The spinon correlation functions, holon order parameter, the decoupling parameter α, and the chemical potential μ can be determined self-consistently.[14,17]

We are now ready to discuss the spin dynamics of the doped triangular antiferromagnet. The AF wave vector in the triangular antiferromagnet is $Q=(\pi/2,\sqrt{3}\pi/2)$. We have performed a numerical calculation for the dynamical spin structure factor $S(Q,\omega)$ and dynamical spin susceptibility $\chi''(Q,\omega)$ of the doped triangular antiferromagnet, and the results of the (a) $S(Q,\omega)$ and (b) $\chi''(Q,\omega)$ spectra at the doping $\delta=0.06$ (dotted line), $\delta=0.09$ (dashed–dotted line), and $\delta=0.12$ (solid line) with the temperature $T=0.1J$ for the parameters $t/J=2.5$ are plotted in Fig. 1. In the correspondence, the results of (a) $S(Q,\omega)$ and (b) $\chi''(Q,\omega)$ spectra at the doping $\delta=0.12$ with the temperature $T=0.1J$ (dotted line), $T=0.3J$ (dashed–dotted line), and $T=0.5J$ (solid line) for the parameters $t/J=2.5$ are plotted in Fig. 2. In comparison with the results of the doped square antiferromagnet,[12] we find that although the spin structure factor spectrum of the doped triangular antiferromagnet still is separated into low- and high-frequency parts in the underdoped and optimally doped regimes, respectively, but the high-frequency part has been depressed due to the strong frustration in the doped triangular antiferromagnet. Moreover, this high-frequency part is suppressed completely in the susceptibility

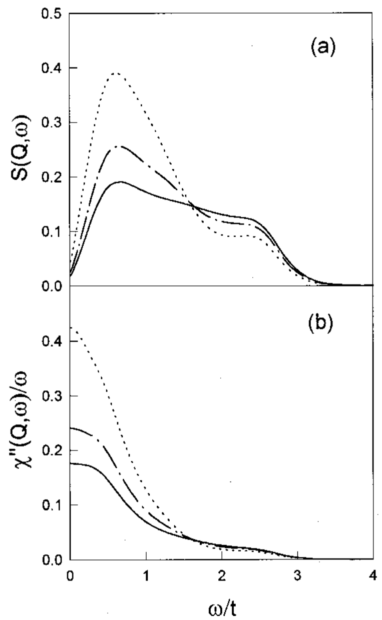

FIG. 1. The dynamical spin structure factor (a) $S(Q,\omega)$ and (b) the dynamical spin susceptibility $\chi''(Q,\omega)$ at the doping $\delta=0.06$ (dotted line), $\delta=0.09$ (dashed–dotted line), and $\delta=0.12$ (solid line) with the temperature $T=0.1J$ for the parameters $t/J=2.5$.

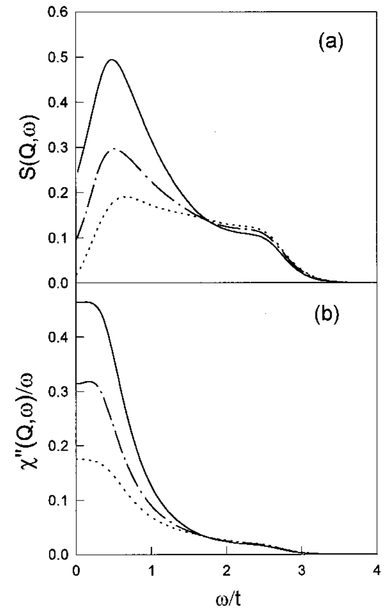

FIG. 2. The dynamical spin structure factor (a) $S(Q,\omega)$ and (b) the dynamical spin susceptibility $\chi''(Q,\omega)$ at the doping $\delta=0.12$ with the temperature $T=0.1J$ (dotted line), $T=0.3J$ (dashed–dotted line), and $T=0.5J$ (solid line) for the parameters $t/J=2.5$.

spectrum. The excitations are rather sharp in the low-frequency range, and the spin structure factor and susceptibility spectra are changed with dopings and temperatures. The low-frequency peaks in the Q point in the spin structure factor and susceptibility spectra are due to the AF fluctuations, which will be in existence even in the undoped case, and therefore dominate the neutron-scattering and NMR processes, while the high-frequency peak in the spin structure factor spectrum may come from the contribution of the free-fermion-like component of the systems, which induces the main effect to the large extent the static spin correlation.

For further understanding the magnetic properties of the doped triangular antiferromagnet in the underdoped and optimally doped regimes, we have discussed the integrated dynamical spin structure factor and integrated dynamical spin susceptibility of the doped triangular antiferromagnet,

$$\bar{S}(\omega,T)=S_L(\omega)+S_L(-\omega)=(1+e^{-\beta\omega})S_L(\omega)$$
$$=(1+e^{-\beta\omega})\frac{1}{N}\sum_k S(k,\omega), \tag{5a}$$

$$I(\omega,T)=\frac{1}{N}\sum_k \chi''(k,\omega). \tag{5b}$$

The numerical results of $\bar{S}(\omega,T)$ at the doping (a) $\delta=0.06$ and (b) $\delta=0.12$ with the temperature $T=0.4J$ (dotted line), $T=0.6J$ (dashed–dotted line), and $T=0.8J$ (solid line) for the parameters $t/J=2.5$ are plotted in Fig. 3. Our results show that in the underdoped and optimally doped regimes, the $\bar{S}(\omega,T)$ is decreased with increasing energies for $\omega<0.6t$, and almost constant for $\omega\geqslant 0.6t$. Moreover, $\bar{S}(\omega,T)$ is essentially temperature independent at the high-frequency range in a wide temperature regime, but in contrast to the case of the doped square antiferromagnet,[12] the heavy deviations occur at the low-frequency range. This temperature dependent behavior of $\bar{S}(\omega,T)$ at the low-frequency range leads to that the shape of the integrated dynamical spin structure factor $\bar{S}(\omega,T)$ does not exhibit a universal behavior. In correspondence with the integrated dynamical spin structure factor, the results of the integrated dynamical spin susceptibility $I(\omega,T)$ at the doping $\delta=0.12$ for the parameter $t/J=2.5$ with the temperature $T=0.2J$ (solid line), $T=0.4J$ (dashed line), and $T=0.6J$ (dashed–dotted line) are plotted in Fig. 4, which show that the shape of the integrated dynamical spin susceptibility also is not universal. In the doped square antiferromagnet,[12] the universal behavior of the integrated dynamical spin structure factor spectrum is closely related with particularly universal behavior of the integrated dynamical spin susceptibility $I(\omega,T)\propto\arctan[a_1\omega/T+a_3(\omega/T)^3]$. But in the present case of the doped triangular antiferromagnet, the temperature dependence of $\bar{S}(\omega,T)$ at the low-frequency range leads to the temperature dependence of the integrated dynamical spin susceptibility at the same

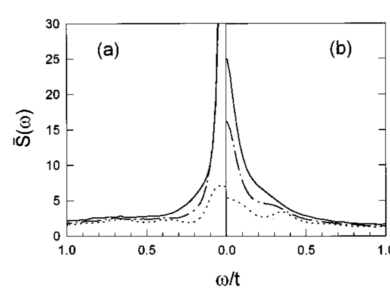

FIG. 3. The integrated dynamical spin structure factor $\bar{S}(\omega)$ at the doping (a) $\delta=0.06$ and (b) $\delta=0.12$ with the temperature $T=0.4J$ (dotted line), $T=0.6J$ (dashed–dotted line), and $T=0.8J$ (solid line) for the parameters $t/J=2.5$.

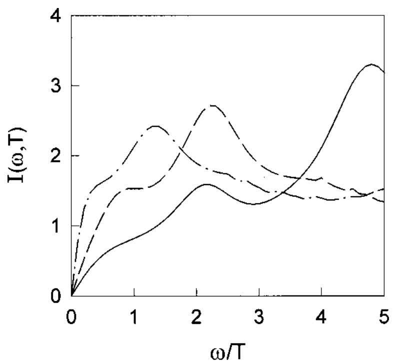

FIG. 4. The integrated dynamical spin susceptibility $I(\omega,T)$ at the doping $\delta=0.12$ for the parameter $t/J=2.5$ with the temperature $T=0.2J$ (solid line), $T=0.4J$ (dashed line), and $T=0.6J$ (dashed–dotted line).

frequency range, and therefore the particularly universal behavior of the integrated dynamical spin susceptibility present in the doped square antiferromagnet, is absent in the doped triangular antiferromagnet.

In the doped square antiferromagnet, it has been shown that there is no normal-state gap in the electronic density of states.[14] In this case, the integrated dynamical spin structure factor is almost temperature independent, and the integrated susceptibility shows the particularly universal behavior[12] as mentioned above. But in the doped triangular antiferromagnet, the electronic density of states has the normal-state gap,[17] which is mainly induced by the frustrated spinons. Since in the charge-spin separation framework the spin dynamics is dominated by the scattering of spinons, which are strongly renormalized because of the strong interactions with fluctuations of surrounding holon excitations. The frustrated spinon moves in the background of the holons, and the cloud of distorted holon background is to follow frustrated spinons, which leads to the anomalous spin dynamics in the doped triangular antiferromagnet. In other words, the normal-state gap due to the frustration is the main reason to cause that the particularly universal behavior of the integrated dynamical spin susceptibility is absent in the doped triangular antiferromagnet in the underdoped and optimally doped regimes.

In summary, we have discussed the spin dynamics of the doped triangular antiferromagnet in the underdoped and optimally doped regimes within the $t-J$ model. We treat the spinon part by using the loop expansion to second order. It is shown that although the dynamical spin structure factor and susceptibility spectra show the anomalous behaviors at the AF zone center, the particularly universal behaviors of the integrated dynamical spin structure factor and susceptibility present in the doped square antiferromagnet, are absent in the doped triangular antiferromagnet.

The authors would like to thank Professor H. Q. Lin and Dr. W. Q. Yu for helpful discussions. The work at Beijing Normal University was supported by the National Natural Science Foundation under Grant No. 19774014. The work at Tamkang University was supported in part by the National Science Council under Grant No. NSC 87-2112-M-023-004.

[1] See, e.g., *Proceedings of Los Alamos Symposium*, edited by K.S. Bedell, D. Coffey, D.E. Meltzer, D. Pines, and J.R. Schrieffer (Addison-Wesley, Redwood City, California, 1990).

[2] P.W. Anderson, Science **235**, 1196 (1987); F.C. Zhang and T.M. Rice, Phys. Rev. B **37**, 3759 (1988).

[3] A.P. Kampf, Phys. Rep. **249**, 219 (1994); M.A. Kastner, R.J. Birgeneau, G. Shiran, and Y. Endoh, Rev. Mod. Phys. **70**, 897 (1998).

[4] B. Keimer, N. Belk, R.J. Birgeneau, A. Cassanho, C.Y. Chen, M. Greven, M.A. Kastner, A. Aharony, Y. Endoh, R.W. Erwin, and G. Shirane, Phys. Rev. B **46**, 14 034 (1992); W.O. Putikka, R.L. Glenister, R.R.P. Singh, and H. Tsunetsugu, Phys. Rev. Lett. **73**, 170 (1994).

[5] B.J. Sternlieb, G. Shirane, J.M. Tranquada, M. Sato, and S. Shamoto, Phys. Rev. B **47**, 5320 (1993); M. Takigawa, A.P. Reyes, P.C. Hammel, J.D. Thompson, R.H. Heffner, Z. Fisk, and K.C. Ott, *ibid.* **43**, 247 (1991); T. Imai, C.P. Slichter, K. Yoshimura, and K. Kosuge, Phys. Rev. Lett. **70**, 1002 (1993); T. Imai, C.P. Slichter, K. Yoshimura, M. Katoh, and K. Kosuge, *ibid.* **71**, 1254 (1993).

[6] S.M. Hayden, G. Aeppli, H. Mook, D. Rytz, M.F. Hundley, and Z. Fisk, Phys. Rev. Lett. **66**, 821 (1991); B. Keimer, R.J. Birgeneau, A. Cassanho, Y. Endoh, R.W. Erwin, M.A. Kastner, and G. Shirane, *ibid.* **67**, 1930 (1991).

[7] J. Rossat-Mignod, L.P. Regnault, C. Vettier, P. Burlet, J.Y. Henri, and G. Lapertot, Physica B **169**, 58 (1991); J. Rossat-Mignod, L.P. Regnault, P. Bourges, P. Burlet, J. Bossy, J.Y. Henri, and G. Lapertot, Physica C **185–189**, 86 (1991).

[8] A.P. Ramirez, R.J. Cava, J.J. Krajewski, and W.F. Peck, Jr., Phys. Rev. B **49**, 16 082 (1994); R.J. Cava, H.W. Zandbergen, A.P. Ramirez, H. Takagi, C.T. Chen, J.J. Krajewski, W.F. Peck, Jr., J.V. Waszczak, G. Meigs, and L.F. Schneemeyer, J. Solid State Chem. **104**, 437 (1993).

[9] A.P. Ramirez, Annu. Rev. Mater. Sci. **24**, 453 (1994); P. Schiffer and A.P. Ramirez, Comments Condens. Matter Phys. **18**, 21 (1996).

[10] J. Jaklič and P. Prelovšek, Phys. Rev. Lett. **74**, 3411 (1995); **75**, 1340 (1995).

[11] E. Dagotto, Rev. Mod. Phys. **66**, 763 (1994), and references therein.

[12] S. Feng and Z. Huang, Phys. Rev. B **57**, 10 328 (1998); Z. Huang and S. Feng, Phys. Lett. A **242**, 94 (1998).

[13] S. Feng, Z.B. Su, and L. Yu, Phys. Rev. B **49**, 2368 (1994); Mod. Phys. Lett. B **7**, 1013 (1993).

[14] S. Feng and Y. Song, Phys. Rev. B **55**, 642 (1997).

[15] L. Capriotti, A.E. Trumper, and S. Sorella, Phys. Rev. Lett. **82**, 3899 (1999).

[16] S. Feng and Z. Huang, Phys. Lett. A **232**, 293 (1997).

[17] Z. Dong and S. Feng, Commun. Theor. Phys. **31**, 509 (1999).